$Ce_4[Si_4O_4N_6]O$—A Hyperbolically Layered Oxonitridosilicate Oxide with an Ordered Distribution of Oxygen and Nitrogen

Elisabeth Irran,[a] Klaus Köllisch,[a] Stefano Leoni,[b] Reinhard Nesper,[b] Paul F. Henry,[c] Mark T. Weller,[c] and Wolfgang Schnick*[a]

Abstract: The yellow-orange oxonitridosilicate oxide $Ce_4[Si_4O_4N_6]O$ was obtained by the reaction of cerium metal with $Si(NH)_2$ and SiO_2 in a radiofrequency furnace at 1560 °C. The crystal structure was determined by single-crystal X-ray diffraction ($a = 1033.67(6)$ pm, $P2_13$, $Z = 4$, $R1 = 0.0412$, $wR2 = 0.0678$) and powder neutron diffraction. In the solid there are complex cations $[Ce_4O]^{10+}$ that are enveloped by a hyperbolical layer structure $[Si_4O_4N_6]^{10-}$. The layer is built up by corner-sharing $SiON_3$ tetrahedra of Q^3 type. The oxygen atoms of the $SiON_3$ tetrahedra are terminally bound to Si, while all nitrogen atoms bridge two neighboring Si centres. The crystallographic differentiation of O and N was unequivocally possible by a careful evaluation of the single-crystal X-ray diffraction data combined with lattice-energy calculations by using the MAPLE concept (Madelung part of lattice energy). Furthermore the results were confirmed by the chemical analyses. Subsequently, the determined N/O distribution and their crystallographic ordering was proved by neutron powder diffraction. In accordance with the molar ratio Si:(O,N) = 2:5 the $[Si_4O_4N_6]^{10-}$ network may be classified as a layer silicate. In this specific case a hyperbolically corrugated topology of the layers is observed; this is correlated to periodic nodal surface (PNS) representatives.

Keywords: cerium · nitrogen · oxygen · silicates · structure elucidation

Introduction

The silicate class of compounds represents one of the most manifold groups of inorganic substances.[1, 2] Among the minerals the oxosilicates play a dominant role and their total mass ratio amounts to nearly 90 weight % from the crust of the earth. Nitridosilicates derive from the classical oxosilicates (which are made up of SiO_4 tetrahedra) by a formal exchange of O against N to yield SiN_4 tetrahedra.[3] This substitution results in a significant extension of the structural possibilities. Unlike the situation of oxosilicates the linkedness (L) of the SiN_4 tetrahedra in nitridosilicates may adopt the values L = (0), 1, or 2. And the coordination number (CN) for nitrogen may vary in the larger range CN(N/Si) = 0, 1, 2, 3, 4 (SiO_4 tetrahedra in oxosilicates: L = 0, 1; CN(O/Si) = 0, 1, 2).[2, 3] However, as compared with the very large number of known oxosilicates only a small number of nitridosilicates have been synthesized so far.[2]

Oxonitridosilicates (so-called "sions") represent an intermediate class of compounds between oxosilicates and nitridosilicates. Similar to the synthetic oxonitridoaluminosilicates (so-called "sialons"),[4] they exhibit desired materials properties like high mechanical hardness and strength, and exceptional thermal and chemical stability. The mineral sinoite, Si_2N_2O, is one of the very few minerals belonging to this class of compounds. It occurs in meteorites or in cosmic dust.[5] Recently, several novel oxonitridosilicates[6a] and oxonitridoaluminosilicates[6b, 6c, 7] have been synthesized and structurally characterized.

A specific problem during the investigation of oxonitridosilicates and oxonitridoaluminosilicates arises from the question of whether the O/N and Al/Si atoms, respectively, are crystallographically ordered, and if so how can this ordering be proved. Due to the very similar atomic form factors of O^{2-}/N^{3-} and Al^{3+}/Si^{4+}, respectively, X-ray diffraction data usually are not appropriate for this differentiation and neutron diffraction experiments have to be performed.

Nearly all nitridosilicates, oxonitridosilicates, and oxonitridoaluminosilicates obtained so far contain highly condensed network structures. Their degree of condensation (i.e.,

[a] Prof. Dr. W. Schnick, Mag. E. Irran, Dipl.-Chem. K. Köllisch
Department of Chemistry, University of Munich (LMU)
Butenandtstrasse 5–13 (house D), 81377 Munich (Germany)
Fax: (+49) 89-2180-7440
E-mail: wolfgang.schnick@cup.uni-muenchen.de

[b] Dr. S. Leoni, Prof. Dr. R. Nesper
Inorganic Solid State Chemistry, ETH Zürich
CH-8092 Zürich (Switzerland)
Fax: (+41) 1-632-1149
E-mail: nesper@inorg.chem.ethz.ch

[c] Dr. P. F. Henry, Prof. Dr. M. T. Weller
Department of Chemistry, University of Southampton
Highfield Southampton, SO17 1BJ (UK)
Fax: (+44) 1703-59-3592
E-mail: mtw@soton.ac.uk

  0947-6539/00/0615-2714 $ 17.50+.50/0

the molar ratio Si:X > 1:2, with X = O, N) usually exceeds the maximum value for oxosilicates (1:4 ≤ Si:O ≤ 1:2).[3] Most of these compounds exclusively contain SiX_4 tetrahedra of Q^4 type, that is, all four X atoms (X = O, N) are bound to two ($O^{[2]}$, $N^{[2]}$),** three ($N^{[3]}$), or even four ($N^{[4]}$) neighboring tetrahedral centers ($Si^{[4]}$).[3] This might be due to the fact that most of these compounds have been synthesized by high-temperature reactions and only the most stable species (i.e., the highly condensed ones) survive the extreme reaction conditions. Consequently these highly condensed compounds exhibit desired materials properties like very low chemical reactivity, high mechanical strength, and thermal stability.[3]

However, lower condensed silicates (molar ratio 1:4 ≤ Si:X ≤ 1:2) are important materials as well. For example, the layer silicates attained relevance as water demineralizing additives and recently they have been used for the preparation of improved polymer nanocomposite materials.[8]

Ideal single-layer silicates exclusively contain SiX_4 tetrahedra of Q^3 type. Their typical degree of condensation amounts to Si:X = 2:5.[1] Pure Q^3 type single-layer silicates with X = N or X = O, N have not been described so far. Here we present the first layered oxonitridosilicate containing only Q^3 type tetrahedra.

Experimental Section

Silicon diimide: In a three-necked bottle CH_2Cl_2 (50 mL, p.a. Merck) was saturated with NH_3 (99.9%, BASF, dried by condensation on sodium and potassium) under dried argon atmosphere. A precooled solution of $SiCl_4$ (20 mL, 0.17 mol, Merck) in CH_2Cl_2 (30 mL) was slowly added with stirring. Afterwards the suspension was carefully warmed to room temperature under NH_3 atmosphere [Eq. (1)]. For purification from NH_4Cl the finely powdered residue was heated in a NH_3 gas flow to 300 °C and finally to 600 °C.[9] The resulting product was a white X-ray amorphous powder with the approximate composition $Si(NH)_2$. It is relatively undefined but very reactive. Silicon diimide is an important precursor compound for the technical production of Si_3N_4 ceramics.[9]

$$SiCl_4 + 6\,NH_3 \xrightarrow{CH_2Cl_2} Si(NH)_2 + 4\,NH_4Cl \quad (1)$$

$Ce_4[Si_4O_4N_6]O$: A mixture of Ce (90.2 mg, 0.6 mmol, Alfa), $Si(NH)_2$ (40.2 mg, 0.7 mmol), and SiO_2 (13.8 mg, 0.2 mmol, Merck) was thoroughly mixed under argon atmosphere in a glove box and transferred into a tungsten crucible positioned in a water-cooled quartz reactor of a radio-frequency furnace.[6c] The reaction mixture was heated under a pure nitrogen atmosphere (purified by silica gel, potassium hydroxide, molecular sieves, P_4O_{10}, and a BTS catalyst) to 850 °C within 5 min, maintained at that temperature for 10 min, heated to 1560 °C within 1 h, kept at this temperature for 2 h, and then slowly cooled to 1200 °C in 62 h. Finally the product was quenched to room temperature. This reaction [Eq. (2)] led to the formation of $Ce_4[Si_4O_4N_6]O$ as yellow-orange, spherical crystals in a yield of approximately 50% among yellow $Ce_3Si_6N_{11}$.[10] The title compound easily can be separated from the byproducts owing to the differing color and the crystal habit.

$$14\,Ce + 5\,SiO_2 + 15\,Si(NH)_2 + 2\,N_2 \xrightarrow[\text{RF furnace}]{1560\rightarrow1200\,^\circ C} 2\,Ce_3Si_6N_{11} + 2\,Ce_4[Si_4O_4N_6]O + 15\,H_2 \quad (2)$$

Energy dispersive X-ray microanalysis (JEOL, JSM-6400) of $Ce_4[Si_4O_4N_6]O$ revealed the molar ratio Ce:Si to a value 4:(4.0–4.1). This is very close to the ideal ratio in the formula $Ce_4[Si_4O_4N_6]O$. Furthermore the exact composition concerning all elements was quantitatively analyzed (Fa. Pascher, Remagen). The determined molar ratio Ce:Si:O:N = 4.0:4.04:5.08:6.08 confirms the composition determined by X-ray and neutron diffraction. The absence of hydrogen (N–H) was checked by IR spectroscopy. Similar to all other nitridosilicates synthesized so far, $Ce_4[Si_4O_4N_6]O$ is stable up to 1600 °C and resistant to hot acid and alkaline solutions.

Crystal structure analysis: X-ray diffraction data were collected on a four-circle diffractometer (Siemens P4). According to the observed reflection conditions (00l with $l = 2n$) of the cubic lattice, the space group $P2_13$ (no. 198) was determined. The unit cell and the space group was verified by a complete set of precession photographs. Additionally all reflections detected by X-ray powder diffractometry (Siemens D5000) of single-phase $Ce_4[Si_4O_4N_6]O$ have been indexed and their observed intensities agree well with the calculated diffraction pattern based on the single-crystal data. The crystal structure of $Ce_4[Si_4O_4N_6]O$ was solved by direct methods by using SHELXTL-Plus[11] and refined with anisotropic displacement parameters for all atoms.

Due to the isoelectronic species N^{3-} and O^{2-} and their very similar atomic form factors the differentiation between both of them by X-ray diffraction methods is not reliable. We therefore developed a structural model of $Ce_4[Si_4O_4N_6]O$ with distinct N and O sites by utilizing a combination of single-crystal X-ray diffraction data and lattice energy calculations obtained by using the MAPLE concept (Madelung part of lattice energy).[12]

An unequivocal experimental discrimination of N and O is possible by neutron diffraction due to the significant difference of their neutron scattering lengths ($b(N) = 9.36 \times 10^{-15}$ m, $b(O) = 5.803 \times 10^{-15}$ m).[13] As no large single crystals of $Ce_4[Si_4O_4N_6]O$ for neutron diffraction could be obtained so far, the N/O distribution was determined by neutron powder diffraction. For the diffraction experiment the time-of-flight method (TOF) was used. About 250 mg of the pure sample were enclosed in a vanadium cylinder. The investigation was performed at the POLARIS instrument at ISIS/Rutherford Appleton Laboratory, Chilton/UK, which due to high flux allows for the measurement of very small samples. Only the data of the back-scattering bank at $2\Theta = 145°$ have been used because of their good resolution and the large d-spacing range. The intensities were normalized against monitor intensities. The Rietveld refinement was performed with the program GSAS[14] by using the X-ray single-crystal data of $Ce_4[Si_4O_4N_6]O$ as a starting model. The Rietveld refinement of the neutron diffraction data gave similar but less accurate atomic coordinates and displacement parameters. Initially O and N were equally located on the same crystallographic anion positions and their occupation factors were dependently refined.

Abstract in German: *Das gelb-orange Oxonitridosilicat-oxid $Ce_4[Si_4O_4N_6]O$ wurde durch Umsetzung von Cer mit $Si(NH)_2$ und SiO_2 im Hochfrequenzofen bei 1560 °C erhalten. Die Kristallstruktur von $Ce_4[Si_4O_4N_6]O$ wurde mittels Einkristall-Röntgenbeugung ($a = 1033.67(6)$ pm, $P2_13$, $Z = 4$, $R1 = 0.0412$, $wR2 = 0.0678$) und Pulver-Neutronenbeugung aufgeklärt. Im Festkörper finden sich komplexe Kationen $[Ce_4O]^{10+}$, die von einer hyperbolisch gewellten Schichtstruktur $[Si_4O_4N_6]^{10-}$ aus eckenverknüpften $SiON_3$-Tetraedern vom Q^3-Typ eingehüllt sind. Die O-Atome der $SiON_3$-Tetraeder sind terminal an Si gebunden, während alle N jeweils zwei benachbarte Si verbrücken. Die kristallographische Unterscheidung von O und N war aufgrund einer sorgfältigen Bewertung der Einkristall-Röntgenbeugungsdaten in Kombination mit gitterenergetischen Berechnungen nach dem MAPLE-Konzept (Madelung Part of Lattice Energy) möglich. Die Ergebnisse wurden auch durch die Elementaranalyse abgesichert. Schließlich wurde die so ermittelte Verteilung N/O und ihre Ordnung vollständig durch Pulver-Neutronenbeugung bestätigt. Entsprechend dem molaren Verhältnis Si:(O,N) = 2:5 des $[Si_4O_4N_6]^{10-}$-Netzwerkes liegt ein Schichtsilicat vor. In diesem speziellen Fall findet sich eine hyperbolisch gewellte Topologie der Schicht, was mit Hilfe von periodischen Knotenflächen (PNS) dargestellt wird.*

[**] The superscripted numbers in square brackets following the element symbols define their coordination numbers.

Relevant crystallographic data and details of the X-ray data collection are shown in Table 1. Table 2 gives the positional and displacement parameters for all atoms. Table 3 lists selected interatomic distances and angles.[15] The Rietveld refinement of the neutron diffraction data is illustrated in Figure 1; the results of the final refinement are summarized in Table 4.

Table 1. Crystallographic data for $Ce_4[Si_4O_4N_6]O$.

formula	$Ce_4Si_4O_5N_6$
M_w [g mol^{-1}]	836.8
crystal system, space group	cubic, $P2_13$ (no. 198)
X-ray powder diffraction	Siemens D 5000
radiation	$Cu_{K\alpha 1}$ ($\lambda = 154.06$ pm, germanium monochromator)
unit-cell dimensions [pm]	$a = 1035.46(6)$
X-ray four-circle diffractometer	Siemens P4
radiation	$Mo_{K\alpha}$ ($\lambda = 71.073$ pm, graphite monochromator)
unit-cell dimensions [pm]	$a = 1033.67(6)$
V [10^6 pm^3]	1104.45
Z	4
ρ_{calcd} [g cm^{-3}]	5.033
$F(000)$	1480
μ [mm^{-1}]	16.63
T [K]	292(2)
crystal size [mm^3]	$0.08 \times 0.08 \times 0.12$
diffraction range [°]	$3 \le 2\theta \le 75$
index range	$-17 \le h, -k, l \le 17$; $-17 \le -h, k, -l \le 17$; octants: 2
scan type	ω
total no. reflections	6706
independent reflections	1940
observed reflections	1940
parameters	62
corrections	Lorentz, polarization, absorption, extinction
absorption correction	empirical (ψ scans)
min./max. transmission ratio	0.066/0.089
Flack parameter x	0.007(33)
min./max. residual electron density [e Å^{-3}]	−1.93/1.85
GOF	1.085
R indices (all data)	$R1 = 0.0412$, $wR2 = 0.0678$
TOF powder diffractometer	POLARIS/ISIS Rutherford Appleton Lab. Chilton (UK)
2θ [°]	145.0
unit-cell dimensions [pm]	$a = 1034.95(3)$
T [K]	292(2)
range [msec]	3–19
no. of data points	3695
no. of observed reflections	1851
refined parameters	39 (structure), 12 (profile)
χ^2	3.00
R indices	$R_p = 0.022$, $wR_p = 0.014$, $R_F = 0.038$

Table 3. Interatomic distances [pm] and angles [°] in the structure of $Ce_4[Si_4O_4N_6]O$ determined by X-ray diffraction with esds in parentheses.

Ce1–O3[1]	237.6 (5)	Si1–O3[1]	166.8 (5)
Ce1–O1[1]	246.2 (3)	Si1–N2[2]	170.3 (5)
Ce1–O3[1]	250.6 (5)	Si1–N1[2]	171.0 (5)
Ce1–O2[0]	252.7 (4)	Si1–N1[2]	171.5 (5)
Ce1–N1[2]	262.0 (6)		
Ce1–N2[2]	262.4 (5)	Si2–O1[1]	165.4 (8)
Ce1–N2[2]	265.6 (5)	Si2–N2[2] 3 ×	169.0 (5)
Ce2–O2[0]	237.2 (14)	N1[2]-Si1-N2[2]	112.0 (3)
Ce2–N1[2] 3 ×	254.6 (5)	N1[2]-Si1-N1[2]	115.9 (3)
Ce2–O3[1] 3 ×	280.8 (15)	N1[2]-Si1-O3[1]	103.5 (3)
		N1[2]-Si1-O3[1]	115.5 (3)
Ce3–N1[2] 3 ×	251.2 (5)	N1[2]-Si1-N2[2]	103.7 (3)
Ce3–O3[1] 3 ×	277.7 (16)	N2[2]-Si1-O3[1]	105.9 (3)
Si1-N1[2]-Si1	123.7 (3)	N2[2]-Si2-O1[1] 3 ×	107.8 (2)
Si1-N2[2]-Si2	163.4 (4)	N2[2]-Si2-N2[2] 3 ×	111.7 (2)

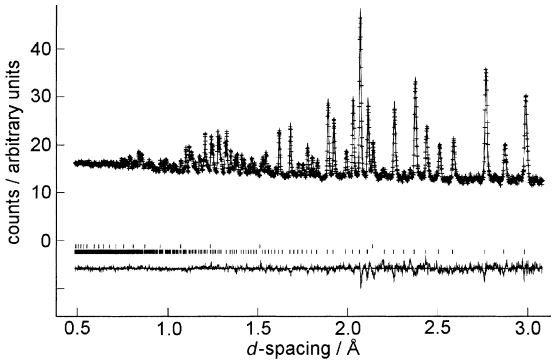

Figure 1. Observed (crosses) and calculated (line) TOF neutron powder diffraction pattern (top) and difference profile (bottom) of the Rietveld refinement obtained with the POLARIS instrument at ISIS/Rutherford Appleton Laboratory, Chilton/UK. The lower row of vertical lines indicates possible peak positions of $Ce_4[Si_4O_4N_6]O$ (upper row: vanadium of the sample container).

Results and Discussion

The title compound is built up of complex tetrahedral cations $[Ce_4O]^{10+}$ and an anionic polymeric network $[Si_4O_4N_6]^{10-}$ that contains only corner sharing $SiON_3$ tetrahedra (Figure 2, Figure 3).[16] Nitrogen, in comparison with oxygen, normally prefers the same[17] or a higher[6c] coordination number towards silicon or aluminum in sions and sialons. This observation is in accordance with Pauling's rules.[18] Therefore, it was anticipated that all nitrogen atoms in $Ce_4[Si_4O_4N_6]O$ each connect

Table 2. Atomic coordinates and anisotropic displacement parameters [pm^2] for $Ce_4[Si_4O_4N_6]O$ determined by single-crystal X-ray diffraction with esds in parantheses. U_{eq} is defined as one third of the trace of the U_{ij} tensor. The anisotropic displacement factor exponent is of the form $-2\pi^2[(ha^*)^2U_{11} + \ldots 2hka^*b^*U_{12}]$.

	x	y	z	FOF[a]	U_{11}	U_{22}	U_{33}	U_{23}	U_{13}	U_{12}	U_{eq}
Ce1	0.81849 (3)	0.70845 (3)	0.03068 (3)	1.0	108 (1)	154 (1)	125 (1)	−43 (1)	0.8 (1)	−6 (1)	129 (1)
Ce2	0.03021 (4)	x	x	0.823 (5)	134 (1)	U_{11}	U_{11}	−3 (1)	U_{23}	U_{23}	134 (1)
Ce3	0.1079 (2)	x	x	0.177 (5)	139 (6)	U_{11}	U_{11}	22 (7)	U_{23}	U_{23}	139 (6)
Si1	0.0749 (2)	0.7548 (2)	0.1952 (2)	1.0	91 (6)	109 (6)	92 (6)	−6 (5)	2 (5)	−2 (5)	97 (3)
Si2	0.4243 (2)	x	x	1.0	94 (4)	U_{11}	U_{11}	−7 (5)	$-U_{23}$	U_{23}	94 (4)
O1	0.3319 (4)	x	x	1.0	150 (14)	U_{11}	U_{11}	29 (14)	$-U_{23}$	U_{23}	150 (14)
O2	0.9073 (6)	x	x	1.0	233 (21)	U_{11}	U_{11}	202 (25)	U_{23}	U_{23}	233 (21)
O3	0.9306 (5)	0.8258 (6)	0.2081 (6)	1.0	95 (17)	450 (34)	364 (29)	−269 (27)	−76 (20)	72 (20)	303 (14)
N1	0.1192 (5)	0.6597 (5)	0.3230 (5)	1.0	181 (21)	132 (20)	95 (18)	40 (16)	−17 (17)	−65 (16)	136 (8)
N2	0.0620 (5)	0.6486 (5)	0.0700 (5)	1.0	182 (23)	164 (22)	99 (18)	−72 (17)	−48 (17)	63 (18)	148 (9)

[a] FOF: fractional occupancy factor.

0947-6539/00/0615-2716 $ 17.50+.50/0 *Chem. Eur. J.* **2000**, *6*, No. 15

Table 4. Atomic coordinates, isotropic displacement parameters [pm^2], and refined fractional occupancy factor (FOF) for $Ce_4[Si_4O_4N_6]O$ determined by neutron powder diffraction with esds in parentheses. U_{eq} is defined as exp $(-8\pi^2 U_{eq} \sin^2\theta/\lambda)$.

	x	y	z	U_{eq}	FOF
Ce1	0.8173(7)	0.7039(5)	0.0312(6)	127(9)	1
Ce2	0.0282(10)	x	x	206(37)	0.65(2)
Ce3	0.1144(13)	x	x	51(47)	0.35(2)
Si1	0.0780(7)	0.7528(6)	0.1961(6)	76(10)	1
Si2	0.4253(6)	x	x	54(16)	1
O1	0.3331(4)	x	x	53(12)	1.03(4)
N1a					−0.03(4)
O2	0.9094(5)	x	x	154(16)	1.08(4)
N2a					−0.08(4)
O3	0.9318(5)	0.8147(5)	0.2132(4)	127(10)	1.07(3)
N3a					−0.07(3)
N1	0.1221(3)	0.6591(3)	0.3231(3)	90(5)	0.98(3)
O1a					0.02(3)
N2	0.0591(3)	0.6450(2)	0.0710(3)	76(4)	0.95(3)
O2a					0.05(3)

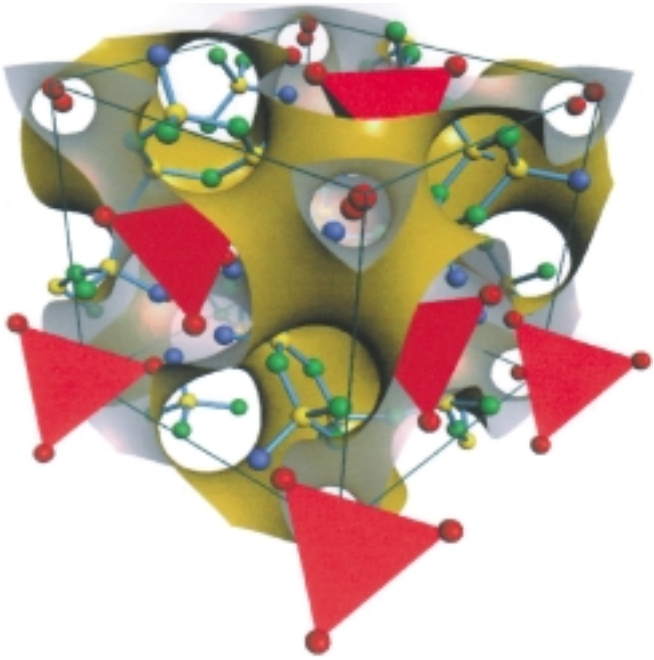

Figure 2. $Ce_4[Si_4O_4N_6]O$ is built up of complex tetrahedral cations $[Ce_4O]^{10+}$ and an anionic polymeric network $[Si_4O_4N_6]^{10-}$ made up of corner-sharing $SiON_3$ tetrahedra; view along [111]. The periodic nodal surface (PNS) FY*xxx* envelops the large tetrahedral cationic complexes $[Ce_4O]^{10+}$. In the region of the upper four vertices of the unit cell the complex cations (displayed as closed red polyhedra) are omitted. The color codes are: Si yellow, N green, O blue, and Ce red.

to two silicon atoms ($N^{[2]}$), while the O atoms are terminally bound to Si or are isolated, respectively ($O^{[1]}$ or $O^{[0]}$).

In order to achieve a crystallographic differentiation of O and N, we performed lattice energy calculations using the Ewald procedure (MAPLE, Madelung part of lattice energy)[12] on the basis of the X-ray single-crystal data. As a common finding of these calculations, the partial MAPLE values for each atom type in a crystal structure varies in a particular range of values (e.g., O^{2-}: 2100–2800 kJ mol^{-1}, N^{3-} 5000–6000 kJ mol^{-1}). Atoms on a specific site, which have been assigned to a wrong atom type (O instead of N or vice versa), normally exhibit a partial MAPLE value that significantly deviates from the characteristic range, thus indicating a false occupation of the regarded position (Table 5). The

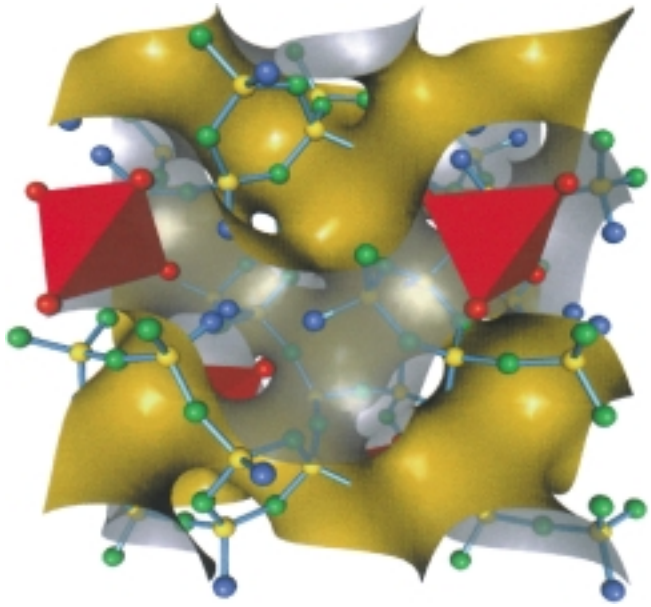

Figure 3. Crystal structure of $Ce_4[Si_4O_4N_6]O$; view along [001]. The entire Si–N substructure extends parallel to the periodic nodal surface (PNS) FY*xxx* and is situated on the yellow side of the surface. Both the cations $[Ce_4O]^{10+}$ and the terminal oxygen atoms of the $SiON_3$ tetrahedra are positioned on the gray side. The Si–O bonds pierce the surface. The color codes are: Si yellow, N green, O blue, and Ce red.

Table 5. Results of the MAPLE calculations for $Ce_4[Si_4O_4N_6]O$ (the partial MAPLE values for an alternative but wrong assignment of O3 as N1 and vice versa are given in brackets). Characteristic partial MAPLE values: N 5000–6000 kJ mol^{-1}, O 2100–2800 kJ mol^{-1}.

	partial MAPLE values [kJ mol^{-1}]
$O1^{[1]}$	2390.6 (2104.2)
$O2^{[0]}$	2084.5 (2051.2)
$O3^{[1]}$	2337.1 (4481.4)
$N1^{[2]}$	5542.7 (3159.7)
$N2^{[2]}$	5458.3 (5528.5)

MAPLE calculations gave strong evidence for a complete ordering of O and N in $Ce_4[Si_4O_4N_6]O$, as expected above.

During the neutron diffraction analysis, both the O and N occupancies were allowed to refine dependently. Starting from a mixed occupation of each position full crystallographic ordering of O and N was proved with refined occupancy factors, which are unity within twice the standard deviations (Table 4). Thus, the neutron diffraction analysis matches exactly with the O/N distribution predicted by the MAPLE calculations on the basis of the single-crystal X-ray data.

The $Si–N^{[2]}$ bond lengths and Si-N-Si bond angles in $Ce_4[Si_4O_4N_6]O$ are in the typical range (169–171.5 pm, 124–163°) for nitridosilicates (Table 3).[3, 6c] As expected, the $Si–O^{[1]}$ bond lengths in the $SiON_3$ tetrahedra are markedly shorter (165–167 pm) than the $Si–N^{[2]}$ bonds.[6c]

The $[Si_4O_4N_6]^{10-}$ network consists of two crystallographically distinct $SiON_3$ tetrahedra centered at Si1 and Si2, respectively. Three $Si1ON_3$ tetrahedra each form a three-membered ring by sharing corners, and cross-linking of these units is accomplished through additional $Si2ON_3$ tetrahedra (Figure 4). All the $SiON_3$ tetrahedra in $Ce_4[Si_4O_4N_6]O$ are of

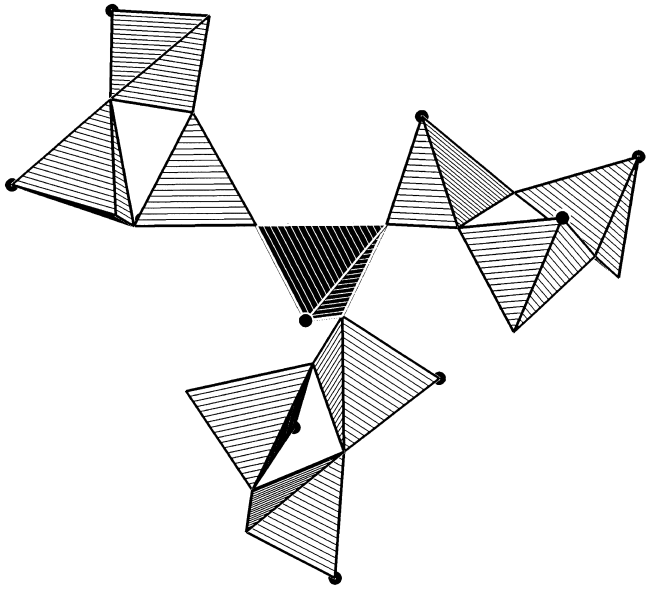

Figure 4. The Si-O-N network structure in $Ce_4[Si_4O_4N_6]O$ is made up of two crystallographically independent $SiON_3$ tetrahedra, centred at Si1 and Si2. The $SiON_3$ units are displayed as closed gray (Si1) and black (Si2) polyhedra. All the nitrogen atoms of the $[Si_4O_4N_6]$ network each connect to two silicon ($N^{[2]}$), while the oxygen (black spheres) are terminally bound to silicon ($O^{[1]}$).

Q^3 type and the molar ratio Si:(N,O) of the network amounts to 2:5. This represents the ideal value of single-layer silicates.[1] Consequently, $Ce_4[Si_4O_4N_6]O$ has to be classified as a layer silicate, though it has cubic crystal symmetry. Normally a cubic structure is not compatible with classical layer silicates, because the latter contain parallel planar sheets of condensed Q^3 type tetrahedra perpendicular to a preferential direction in space. However, in $Ce_4[Si_4O_4N_6]O$ the sheets are hyperbolically corrugated and not planar. Classical layer silicates only contain Si_nO_n rings. In contrast to this the Si-O-N substructure of $Ce_4[Si_4O_4N_6]O$ exhibits closed rings, but infinite helices of alternating Si and N as well. These last (e.g., 2_1 helices running along [100]) become apparent, if the neighboring Si centres of the $SiON_3$ tetrahedra are directly connected (Figure 5). The frequency distribution of Si_nN_n ring sizes per unit cell of $Ce_4[Si_4O_4N_6]O$ (i.e., the cycle-class sequence[19] for $n = 1,2,3,4\cdots$) amounts to {-,0,4,0,0,0,0,0,0,0,0, 0,0,0,12,60,120$\cdots$}. Accordingly the smallest closed loops in the $[Si_4O_4N_6]$ substructure are Si_3N_3 and $Si_{15}N_{15}$ rings, respectively (Figure 5). The occurence of three-membered rings in $Ce_4[Si_4O_4N_6]O$ is in contrast to the structures of most layer silicates.[1] Due to the electrostatic repulsion of the SiO_4 tetrahedra such small rings are not favored in oxosilicates; however, in the less ionic nitridosilicates they occur frequently.[3]

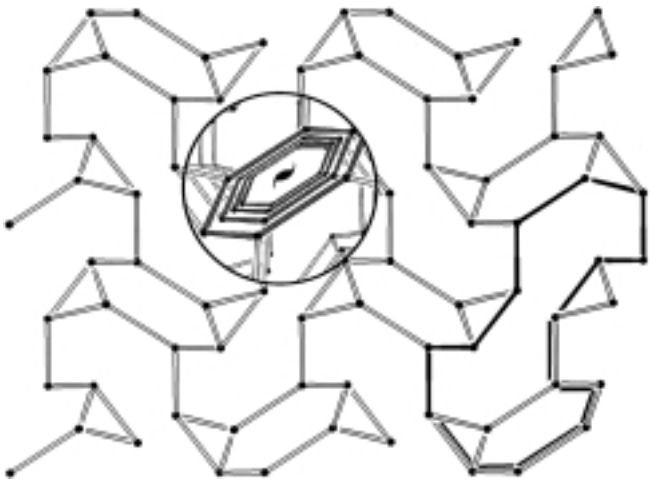

Figure 5. Topological representation of the Si-O-N network structure in $Ce_4[Si_4O_4N_6]O$; view along [100]. The O and N atoms are omitted and neighboring Si centres are directly connected. The network contains small Si_3N_3 rings, large $Si_{15}N_{15}$ rings (emphasized by bold lines), and furthermore infinite 2_1 helices of alternating Si and N atoms running along [100]; enlarged perspective representation within the circle.

The unequivocal proof of a hyperbolical layer structure in $Ce_4[Si_4O_4N_6]O$ and its graphical representation elegantly was possible using periodic surface representations.[20, 21] Amongst several other structures the zeolites are prominent examples of periodic hyperbolic frameworks that have been described by periodic minimal surfaces (PMS) and by periodic nodal surfaces (PNS).[22, 23] Similarly the three-dimensional framework structures in intermetallic compounds develop according to PMS and PNS as well.[21, 24, 25]

In $Ce_4[Si_4O_4N_6]O$ a hyperbolically corrugated layer following the shape of a periodic nodal surface (PNS) was identified. The space group $P2_13$ (no. 198) of the title compound allows for a transition between frameworks of face-centred (F) and of triply branched (Y) character. This is reflected in the point configuration FY*xxx* (Wyckoff positions 4a and 12b), characteristic for this space group.[26] In the PNS approach a short Fourier series, consisting of coefficients with indices *hkl*, amplitudes $|S|$, and phases α, is utilised to generate a symmetry-adapted topological representation of the space-group characteristics. In this case the Fourier coefficients with the indices 110 and 111 allow the generation of the Y and F topology, respectively. Although, because of their permutation behavior they belong to the higher Laue class (*m*3*m*) and thus to higher space groups, their combined use allows the generation of a topology that is typical for the space group $P2_13$. It may reflect the transition from an F to a Y characteristic and vice versa, according to the choice of the actual amplitudes and actual phases.

The PNS FY*xxx*,[27] generated by S_1 (*hkl*: $110\,|\,S_1 = 1\,|\,\alpha_1 = -\pi/2$) and S_2 (*hkl*: $111\,|\,S_2 = 2\,|\,\alpha_2 = -\pi/4$) describes the topological situation of $Ce_4[Si_4O_4N_6]O$ very well (Figures 2 and 3). This PNS separates the whole structure into two independent spaces. Thus, topologically there is no path from the yellow side of the PNS to its gray side (see Figures 2 and 3). In $Ce_4[Si_4O_4N_6]O$ the entire Si–N substructure extends parallel to this PNS and it is situated on the yellow side of the surface, while both the cations $[Ce_4O]^{10+}$ and the terminal

0947-6539/00/0615-2718 $ 17.50+.50/0 *Chem. Eur. J.* **2000**, *6*, No. 15

oxygen atoms of the $SiON_3$ tetrahedra are positioned on the gray side. The Si–O bonds pierce the surface (Figure 3).

In classical layer silicates an infinite number of parallel sheets occur. The single layers are not directly connected by Si-O-Si bonds, but they are separated by cations and/or intercalated species. In contrast to that in $Ce_4[Si_4O_4N_6]O$ there is only one hyperbolical layer of corner-sharing $SiON_3$ tetrahedra and all of the tetrahedra belong to this single layer. For this reason intercalation into $Ce_4[Si_4O_4N_6]O$ probably is not favorable.

Presumably the hyperbolical modulation of the $[Si_4O_4N_6]$ substructure is caused by the $[Ce_4O]^{10+}$ cations. Unlike other large complex cations (e.g., tetraalkylammonium), $[Ce_4O]^{10+}$ exhibits a very high charge density forcing the $[Si_4O_4N_6]$ layer to envelop the complex cations (Figures 2 and 3) and preventing the adoption of planarity.

As expected the Ce···O distances (237 pm) within the complex cations $[Ce_4O]^{10+}$ are shorter as compared with the Ce···O[1] (238–280 pm) and Ce···N[2] distances (251–266 pm) towards the N/O atoms of the $[Si_4O_4N_6]$ network. The crystallographically independent Ce sites are coordinated by six or seven N/O atoms, respectively. The observed distances correspond well with the sum of the ionic radii.[28, 29]

One vertex atom of the $[Ce_4O]^{10+}$ ions is distributed between the neighboring split positions Ce2 and Ce3. This disorder has been confirmed independently by the refinement of the diffraction data sets of three individual single-crystals and also by the neutron powder diffraction. However, the determined occupancy factors considerably differ between the X-ray (Ce2:Ce3 $\approx$ 5/6:1/6) and the neutron refinement (4/6:2/6; neutron scattering length $b(\mathrm{Ce}) = 4.84 \times 10^{-15}$ m).[13] At present this cannot be explained. However in terms of the structural considerations it does not seem to be very important, because the two split positions Ce2 and Ce3 both match well with the surrounding neighboring atoms: The displacement ellipsoids of O2, O3 (first neighboring shell), and Ce1 (second neighboring shell) impressively show the correlated switching as illustrated in Figure 6. If Ce3 is occupied O3 will move closer towards this site, while the opposite O3 displacement approaches the Ce2 site (Figure 6). Bond-valence-sum calculations[30] indicate that in an opposite way O2 moves away from the Ce2 site if Ce2 is occupied, otherwise a too short Ce2–O2 bond length of 196 pm would occur. However, no convincing split models for O2 and O3 could be refined and the best results were obtained with a severe anisotropic displacement of both oxygen positions. The bond lengths Ce–O mentioned in the structural discussion in each case refer to the appropriate split position of O2 and O3.

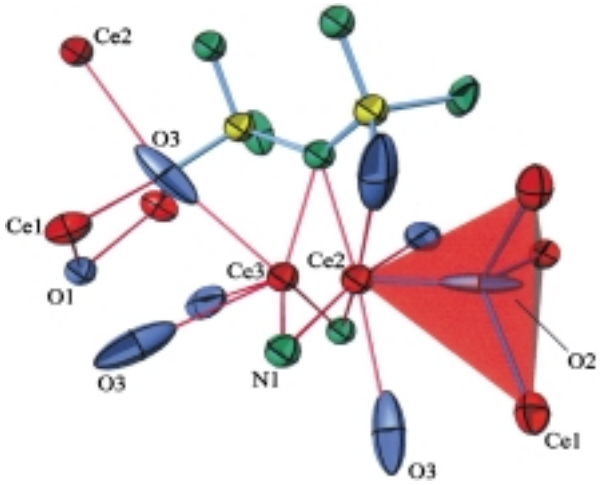

Figure 6. Local environment of the partially occupied positions Ce2 and Ce3. The anisotropic thermal displacement ellipsoids (90%) of O2 and O3 demonstrate the switching of these atoms depending on the occupancy of the Ce2 and Ce3 positions, for details see text; view along [100]. The color codes are: Si yellow, N green, O blue, and Ce red.

Presumably, the Ce1 positions feel the actual location of O2 as well, but their displacement is fairly small because the O2 movement is nearly perpendicular with respect to the Ce1–O2 vector (Figure 6). This argumentation shows quite well that both Ce2 and Ce3 are reasonable sites. The switching of cerium between both sites only influences the local environment.

For a possible Ce2/Ce3 ordering that maintains cubic symmetry (a likely though not a necessary conjecture) the observed occupancies (Ce2:Ce3 = 5:1 or 4:2 per unit cell) and the fact that the lowest multiplicity of sites in cubic systems is four have to be considered. Thus the simplest cubic solution would lead to at least an eightfold unit cell, that would have either 40 Ce2 + 8 Ce3 or 32 Ce2 + 16 Ce3. Such an ordered superstructure might be observable, but the driving force towards this long-range ordering may be weak due to the excellent local adjustment to the actual occupation of the Ce2 and Ce3 sites, as outlined above. On the other hand, this disorder may be indicative for a possible high-temperature modification of $Ce_4[Si_4O_4N_6]O$. However, experimental evidence for a phase transition has not yet been obtained.

In Figure 2 the split positions Ce2/Ce3 neighboring the upper four vertices of the unit cell are displayed, while the complex cations $[Ce_4O]^{10+}$ (represented by red, closed tetrahedra) are omitted in that region. Apparently the two split positions develop along the tunnel structure of the PNS and thus parallel to the Si–N network. As shown by analysis of the displacement ellipsoids (see above) this allows for a flip-flop between Ce2 and Ce3 without disturbing the Si–N network too much.

In the Ce/Si/O/N system we recently obtained a second quaternary phase, $Ce_{16}Si_{15}O_6N_{32}$. This oxonitridosilicate crystallizes with a superstructure of a distorted defect perovskite variant that contains SiN_6 octahedra and $Si(O,N)_4$ tetrahedra.[6a] Relative to $Ce_{16}Si_{15}O_6N_{32}$, the title compound $Ce_4[Si_4O_4N_6]O$ (= $Ce_{16}Si_{16}O_{20}N_{24}$) contains a significantly higher amount of oxygen. This might be the reason for the formation of extra network $(O^{[0]})^{2-}$ that are not directly connected to Si.

The N-containing melilites $Ln_2Si_3O_3N_4$ and $Ln_2Si_{2.5}Al_{0.5}O_{3.5}N_{3.5}$ (Ln = lanthanoides) in principle are layered silicates with planar silicate sheets.[6b, 31] However besides Q^3 type tetrahedra there also occur Q^4 tetrahedra.

Conclusion

The oxonitridosilicate oxide $Ce_4[Si_4O_4N_6]O$ is the first representative of a hyperbolic layer silicate. Lattice-energy calculations obtained by using the MAPLE concept based on

single-crystal X-ray structural data allowed for the differentiation between O and N in this oxonitride. The results have been confirmed independently by neutron diffraction experiments. According to our experience the results of the MAPLE calculations clearly indicate, if there is a crystallographic ordering of N and O. As an example to prove the opposite the MAPLE results for the N-containing melilites $Sm_2Si_3O_3N_4$ and $Ln_2Si_{2.5}Al_{0.5}O_{3.5}N_{3.5}$ (Ln = Ce, Pr, Nd, Sm, Gd) are not indicative for a crystallographic ordering of O/N and Al/Si.[6b] This is in agreement with the neutron diffraction results.[31]

In the meantime we have investigated the novel sialons $Sr_3Ln_{10}Si_{18}Al_{12}O_{18}N_{36}$ (Ln = Ce, Pr, Nd) by single-crystal X-ray diffraction and powder neutron diffraction. Again the crystallographic ordering of O/N and Al/Si, which was derived from the MAPLE calculations, is in agreement with the neutron diffraction results.[32]

Acknowledgement

The authors would like to thank the Fonds der Chemischen Industrie, the Bundesministerium für Bildung, Wissenschaft und Forschung (bmb + f) (Germany), project 03-SC5LMU-5, and especially the Deutsche Forschungsgemeinschaft (Schwerpunktprogramm Nitridobrücken and Gottfried-Wilhelm-Leibniz-Programm) for generous financial support.

[1] F. Liebau, *Structural Chemistry of Silicates*, Springer, Berlin, **1985**, pp. 14.
[2] F. Liebau, *Angew. Chem.* **1999**, *111*, 1845; *Angew. Chem. Int. Ed.* **1999**, *38*, 1733.
[3] W. Schnick, H. Huppertz, *Chem. Eur. J.* **1997**, *3*, 679.
[4] a) C. M. Sheppard, K. J. D. MacKenzie, M. J. Ryan, *J. Eur. Ceram. Soc.* **1998**, *18*, 185; b) C. C. Anya, A. Hendry, *J. Mater. Sci.* **1994**, *29*, 527; c) C. C. Anya, A. Hendry, *J. Eur. Ceram. Soc.* **1994**, *13*, 247.
[5] M. Wada, A. Inoue, S. Okutani, E. Sakamoto, K. Takahashi, M. Okano, K. Izumo, T. Katou, H. Kumagal, M. Nishida, Y. Tendow, M. Shima, H. Yabuki, A. Okada, S. Yabuki, H. Nakatani, Y. Chiba, N. Tazima, S. Moriuchi, R. Sakamoto, K. Fujitaka, S. Abe, K. Aral, I. Urabe, K. Yamasaki, T. Tsujimoto, T. Yoshimoto, K. Okamoto, K. Katsurayama, I. Aoyama, F. Tohyama, *Rep. Inst. Phys. Chem. Res.* **1983**, *59*, 1.
[6] a) K. Köllisch, W. Schnick, *Angew. Chem.* **1999**, *111*, 368; *Angew. Chem. Int. Ed.* **1999**, *38*, 357; b) R. Lauterbach, W. Schnick, *Z. Anorg. Allg. Chem,* **1999**, *625*, 429; c) W. Schnick, H. Huppertz, R. Lauterbach, *J. Mater. Chem.* **1999**, *9*, 289.
[7] a) R. Lauterbach, W. Schnick, *Z. Anorg. Allg. Chem.* **1998**, *624*, 1154; b) R. Lauterbach, W. Schnick, *Z. Anorg. Allg. Chem,* **2000**, *626*, 56.
[8] C. Zilg, P. Reichert, F. Dietsche, T. Engelhardt, R. Mülhaupt, *Kunststoffe* **1998**, *88*, 1812.
[9] H. Lange, G. Wötting, G. Winter, *Angew. Chem.* **1991**, *103*, 1606; *Angew. Chem. Int. Ed. Engl.* **1991**, *30*, 1579.
[10] T. Schlieper, W. Schnick, *Z. Anorg. Allg. Chem.* **1995**, *621*, 1535.
[11] G. M. Sheldrick, *SHELXTL-Plus*, *V 5.0*, Crystallographic System, Siemens Analytical X-Ray instruments, Madison, WI, **1994**.
[12] a) R. Hoppe, *Angew. Chem.* **1966**, *78*, 52; *Angew. Chem. Int. Ed. Engl.* **1966**, *5*, 95; b) R. Hoppe, *Angew. Chem.* **1970**, *82*, 7; *Angew. Chem. Int. Ed. Engl.* **1970**, *9*, 25.
[13] V. F. Sears, *Neutron News* **1992**, *3*, 26.
[14] R. B. von Dreele, A. C. Larson , General Structure Analysis System, Los Alamos National Laboratory, Report LAUR 86–748, **1990**.
[15] Further details on the crystal structure investigations may be obtained from the Fachinformationszentrum Karlsruhe, 76344 Eggenstein-Leopoldshafen, Germany (fax: (+49) 7247-808-666; e-mail: crysdata @fiz-karlsruhe.de), on quoting the depository numbers CSD-410925 (X-ray data) and CSD-410926 (neutron data).
[16] Oxocentred tetrahedra $[M_4O]$ have been identified frequently, for an overview see: S. V. Krivovichev, S. K. Filatov, T. F. Semenova, *Russ. Chem. Rev.* **1998**, *67*, 137.
[17] A. Koroglu, D. C. Apperley, R. K. Harris, D. P. Thompson, *J. Mater. Chem.* **1996**, *6*, 1031.
[18] L. Pauling, *The Nature of the Chemical Bond*, 3rd ed., Cornell University Press, Ithaca, New York, **1960**, p. 543.
[19] W. E. Klee, *Z. Kristallogr.* **1987**, *179*, 67.
[20] H. G. von Schnering, R. Nesper, *Z. Phys. B* **1991**, *83*, 407.
[21] S. Leoni, Ph.D. Thesis, ETH Zurich, **1998**.
[22] H. G. von Schnering, R. Nesper, *Angew. Chem.* **1987**, *99*, 1097; *Angew. Chem. Int. Ed. Engl.* **1987**, *26*, 1059.
[23] L. Faelth, S. Andersson, *Z. Kristallogr.* **1982**, *160*, 313.
[24] A. Zürn, Ph.D. Thesis, MPI Stuttgart, **1998**.
[25] Yu. Grin, U. Wedig, H. G. von Schnering, *Angew. Chem.* **1995**, *107*, 1318; *Angew. Chem. Int. Ed. Engl.* **1995**, *34*, 1204.
[26] *International Tables for Crystallography*, (Ed.: T. Hahn), Kluwer Academic, Dordrecht, **1996**.
[27] The choice of $\alpha = -\pi/4$ leads to a total symmetry according to $P4_332$, but any phase shift off this value leads back to $P2_13$.
[28] W. H. Baur, *Crystallogr. Rev.* **1987**, *1*, 59.
[29] R. D. Shannon, C. T. Prewitt, *Acta Crystallogr. Sect. B* **1969**, *25*, 925.
[30] N. E. Brese, M. O'Keeffe, *Acta Crystallogr. Sect. B* **1991**, *47*, 192.
[31] P. L. Wang, P. E. Werner, *J. Mater. Sci.*, **1997**, *32*, 1925.
[32] R. Lauterbach, E. Irran, P. F. Henry, M. T. Weller, W. Schnick, *J. Mater. Chem.* **2000**, *10*, 1357.

Received: November 8, 1999
Revised version: March 8, 2000 [F2123]

  0947-6539/00/0615-2720 $ 17.50+.50/0